Z-99 MULTIVALUED OPERATORS: LIMITATIONS AND IMPROVEMENTS

M.O. FRIJLINK and C.P.A.WAPENAAR
Section of Applied Geophysics, Centre for Technical Geoscience, Delft University of Technology, The Netherlands

Introduction

It is well-known that Kirchhoff migration, using only the first arrivals in the Green's functions, may lead to significant artifacts in the migration output when the macro velocity model is complex [2]. In many cases the amplitudes of the later arrivals in multivalued Green's functions are higher than the amplitudes of the first arrivals. Hence, employing the arrival with the strongest amplitude rather than the first arrival may already give significant improvements. Of course employing all arrivals gives the best result that can be obtained with Kirchhoff migration. However, it is a common misconception that this "best result" is the correct result. Here we do not refer to the fact that ray-traced multivalued Green's functions are high frequency approximations of the exact Green's functions, nor do we refer to the negligence of evanescent waves. We claim that even application of the Kirchhoff-Helmholtz integral with exact back-propagating Green's functions may give rise to amplitude errors that are of the same order of magnitude as those caused by ignoring the later arrivals in multivalued Green's functions. In the following we first demonstrate this with a numerical example, then we give an explanation and finally we demonstrate a solution.

Downward extrapolation with single- and multivalued operators

In order to analyse the limitations of multivalued operators we consider a symmetric syncline model with a large impedance contrast (Figure 1a), $c_1 = 1500\,m/s$, $\rho_1 = 1500\,kg/m^3$, $c_2 = 3000\,m/s$, and $\rho_2 = 3000\,kg/m^3$. A plane wave source with finite length at depth level $z_S = 520$m radiates an upgoing wave field, which is registered at the surface $z_0 = 0$, see Figure 1b. The minimum and maximum frequencies of the source spectrum are 12.75 Hz and 34.75 Hz, respectively. Our aim is to downward extrapolate this upgoing wave field back to the source level z_S. To this end we modeled Green's functions for a range of source points at this depth level. The Green's function related to the source point at the symmetry axis of the syncline model, is shown in Figure 1c. To avoid discussions about the accuracy of the Green's functions, we modeled them using a finite difference method; the source spectrum is flat between 12.75 Hz and 34.75 Hz. Note that the first arrival in this Green's function is weaker than the later arrival. Applying downward extrapolation, using only the first arrival of the Green's function, yields the result shown in Figure 2a. The left and right parts clearly resemble the plane wave source, however, the central part is largely distorted. The results of downward extrapolation, using the strongest arrival and all arrivals, respectively, are shown in Figures 2b and 2c. These results clearly look better than the result in Figure 2a, but the collected amplitude cross-sections (Figure 2d) reveal that the amplitudes are overall too low and significantly distorted in the middle of the section. In this figure and in all other amplitude cross sections the solid gray line corresponds to the source function. Before we explain the discrepancies, we show the results of two other methods, reverse time extrapolation [4], see Figure 3a, and recursive explicit depth extrapolation [3, 6], see Figure 3c. The reverse time extrapolation amplitude cross-section in Figure 3b is very similar to that of the Kirchhoff method with the multivalued Green's function (Figure 2d). This confirms the observation by Esmersoy [1] that reverse time extrapolation is equivalent with the Kirchhoff-Helmholtz integral with back-propagating Green's functions. The amplitudes of recursive depth extrapolation, Figure 3d, also deviate significantly from the correct result.
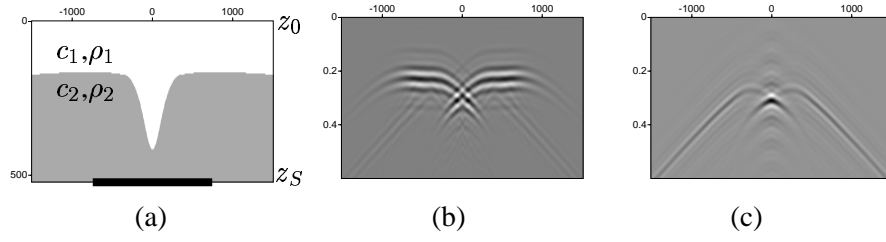
Figure 1: (a) Syncline model. (b) Plane wave response. (c) Multivalued operator (Green's function)
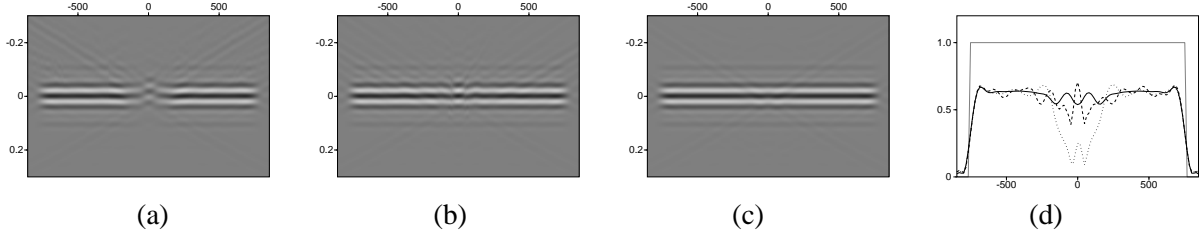

Figure 2: Kirchhoff downward extrapolation results. (a) Using the first arrivals only. (b) Using the strongest arrivals only. (c) Using all arrivals of the multivalued operator. (d) Amplitude cross-sections of the downward extrapolation results of Figure 2a, dotted, 2b, dashed, and 2c, solid black, respectively. Solid gray corresponds to the source amplitude.

Explanation of the limitations of the multivalued operator

The explanation for the amplitude errors of Kirchhoff extrapolation with multivalued operators (Figure 2d) is that the Kirchhoff-Helmholtz integral with back-propagating Green's functions is exact only when applied to a closed surface, that is when all energy scattered by the interface is accounted for, transmission as well as reflection. The seismic acquisition surface is always an open surface, so part of the energy is neglected.
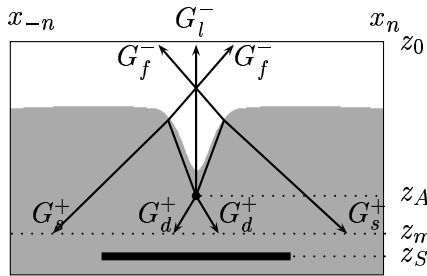

Figure 4: Multivalued Green's function in a syncline model.

We have illustrated the situation in Figure 4. The closed surface consists of the acquisition surface at z_0, a boundary in the subsurface at z_m, between the Green's source point at depth level z_A and the plane wave source at depth level z_S, and vertical boundaries at $x_{\pm n}$. The z-coordinates obey $z_0 < z_A < z_m < z_S$; note that in the examples in the previous section we have taken the limits $z_A \downarrow z_m$ and $z_S \uparrow z_m$. In a previous study [8] we showed that in inhomogeneous media the Green's function as well as the data consists of two parts; transmitted parts arriving as an upgoing wave at the acquisition surface z_0, G_t^- and P_t^-, and reflected parts at z_m, G_s^+ and P_s^+, propagating downward through the subsurface. In complex velocity models the situation is even more complicated; then G_t^- contains multivalued arrivals, first arrivals G_f^- and later arrivals G_l^-. It is clear that Kirchhoff migration schemes with multivalued operators account for the transmitted fields, G_f^- and G_l^- at z_0. In practice the reflections at z_m and $x_{\pm n}$ cannot be taken into account because no data are available at these boundaries; for $x_{\pm n} \rightarrow \pm\infty$ the integrals over the vertical boundaries go to zero, but the contribution from z_m cannot be neglected. This explains the discrepancy between the gray reference curve and the other curves in Figure 2d. To illustrate this, we model the data at z_m and $x_{\pm n}$ and we evaluate the Kirchhoff-Helmholtz integral along these boundaries. Next we add this result to that of Figure 2c, i.e., to the result of the Kirchhoff-Helmholtz integral with the upgoing Green's functions G_f^- and G_l^- at z_0. The result of this addition is shown in Figure 5a. Apart from the fact that now also the downgoing wave field is reconstructed, the amplitude of the upgoing wave is improved. This is confirmed in Figure 5b which shows that the amplitude cross-section of Figure 5a (the dashed line) accurately matches the amplitude cross-section of the original upgoing plane wave field.

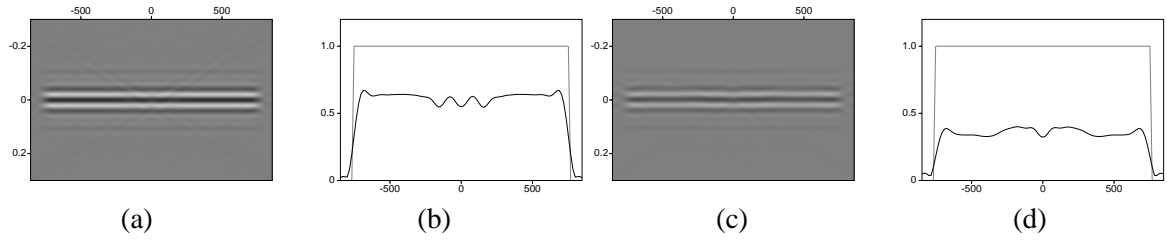(a)   (b)   (c)   (d)

Figure 3: (a) Reverse time extrapolation. (b) Amplitude cross-section of 3a. (c) recursive explicit depth extrapolation. (d) Amplitude cross-section of 3c
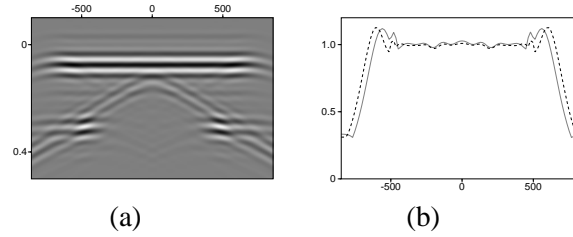

(a)   (b)

Figure 5: (a) Sum of the Kirchhoff-Helmholtz integral over the upper boundary (Figure 2c) the lower boundary (Figure 5a), and the two boundaries at $x_{\pm n}$. (b) Amplitude cross-section of figure (a) (dashed) and the reference amplitudes (solid gray).

Iterative downward extrapolation

In the previous section we showed that true amplitude extrapolation requires the evaluation of the Kirchhoff-Helmholtz integral along a closed boundary. Here we discuss an iterative downward extrapolation method, which avoids the integral along the lower and side boundaries, but instead uses the reflectivity information in the data. For inverse wave field extrapolation through finely layered media, we previously derived the following expression [7]

$$\mathbf{I} - \mathbf{R}_0^\dagger(z_0)\mathbf{R}_0(z_0) = \{\mathbf{W}_g^+(z_m, z_0)\}^\dagger \mathbf{W}_g^+(z_m, z_0), \tag{1}$$

where $\mathbf{W}_g^+(z_m, z_0)$ is the forward extrapolation matrix for flux-normalized downgoing waves between depth levels z_0 and z_m, $\mathbf{R}_0(z_0)$ is the flux-normalized reflection response matrix of the subsurface measured at z_0 (assuming there is no free surface); corresponding columns of $\mathbf{W}_g^+(z_m, z_0)$ and $\mathbf{R}_0(z_0)$ describe the transmission-response at z_m and reflection-response at z_0, resulting from a single point-source at one of the receiver-posistions. The subscript $_g$ stands for generalized primary, which we used to denote that all internal multiples of the finely layered medium are included and † denotes transposition and complex conjugation. However, since the derivation was for arbitrarily inhomogeneous media, we may apply this expression as well for complex media with strong lateral variations, like the syncline model in Figure 1a. Hence, we extend the definition of generalized primary to include multivalued arrivals as well. A final note on (1) should be that each of the diagonal elements of this matrix-equation formulates energy conservation; the diagonal elements of left and right-hand sides of (1) read

$$\left[\mathbf{I} - \mathbf{R}_0^\dagger\mathbf{R}_0\right]_{qq} = 1 - \sum_p R_{0,pq}^* R_{0,pq}, \tag{2}$$

$$\left[\{\mathbf{W}_g^+\}^\dagger\mathbf{W}_g^+\right]_{qq} = \sum_p W_{g,pq}^* W_{g,pq}. \tag{3}$$

From (1) we obtain

$$\{\mathbf{F}_g^-(z_m, z_0)\}^T = \mathbf{F}_g^+(z_0, z_m) = \left(\mathbf{I} - \mathbf{R}_0^\dagger(z_0)\mathbf{R}_0(z_0)\right)^{-1}\{\mathbf{W}_g^+(z_m, z_0)\}^\dagger, \tag{4}$$

where $\mathbf{F}_g^-(z_m, z_0)$ is the inverse extrapolation matrix for flux-normalized upgoing waves between depth levels z_m and z_0, and ^{T} denotes transposition. Applying a Neumann expansion and using the properties

$\{\mathbf{W}_g^+(z_m, z_0)\}^T = \mathbf{W}_g^-(z_0, z_m)$ and $\mathbf{R}_0^T(z_0) = \mathbf{R}_0(z_0)$, equation (4) becomes

$$\langle \mathbf{F}_g^-(z_m, z_0)\rangle^{(k)} = \{\mathbf{W}_g^-(z_0, z_m)\}^\dagger \sum_{i=0}^{k} \Big[\mathbf{R}_0(z_0)\mathbf{R}_0^*(z_0)\Big]^i, \tag{5}$$

where $\langle \cdot \rangle^{(k)}$ denotes the kth order estimate. Each column of the matrix $\mathbf{W}_g^-(z_0, z_m)$ contains a discretized flux-normalized version of $G_f^- + G_l^-$ at $x_{3,0}$, for a specific source position at z_m. Hence in this notation the Kirchhoff integral with back-propagating multivalued Green's functions reads

$$\langle \mathbf{P}^-(z_m)\rangle^{(0)} = \{\mathbf{W}_g^-(z_0, z_m)\}^\dagger \mathbf{P}^-(z_0), \tag{6}$$

where $\mathbf{P}^-(z_0)$ and $\mathbf{P}^-(z_m)$ are vectors containing the discretized upgoing wave fields at depth levels z_0 and z_m, respectively. The superscript $^{(0)}$ denotes the zeroth order estimation. Using the operator of equation (5), the kth order estimation reads

$$\langle \mathbf{P}^-(z_m)\rangle^{(k)} = \{\mathbf{W}_g^-(z_0, z_m)\}^\dagger \sum_{i=0}^{k} \Big[\mathbf{R}_0(z_0)\mathbf{R}_0^*(z_0)\Big]^i \mathbf{P}^-(z_0). \tag{7}$$

Note that indeed only input data at z_0 is required and that the correction terms can be fully obtained from the deconvolved reflection measurements at z_0. Results for $k=0$ and 2 are shown in Figures 6a and b. The cross-sections in Figure 6c show that the results converge to the correct amplitudes.
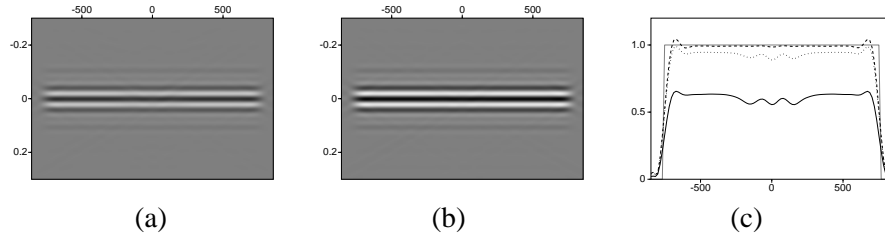

(a) (b) (c)

Figure 6: Downward extrapolation results, using equation (7). (a) $k = 0$. (b) $k = 2$. (c) Amplitude cross-sections for $k = 0$, solid, $k = 2$, dotted, and $k = 10$, dashed.

Conclusions

Kirchhoff migration, using only the first arrivals in the Green's functions, may lead to significant artifacts in the migration output when the macro velocity model is complex [2]. However, we demonstrated that even application of the Kirchhoff-Helmholtz integral with multivalued back-propagating Green's functions may give rise to significant laterally varying amplitude errors, particularly when the contrasts in the medium are large. The explanation lies in the fact that backscattered energy should be taken into account as well.

We derived an inverse extrapolation operator (5) that accounts for the multivaluedness of the Green's functions as well as for the scattering losses related to the contrasts in the medium. The correction term is derived directly from the reflection measurements. Since our method leads to an inverse operator rather than a time-reversed one, it provides an alternative to the inversion method proposed by Ten Kroode et al. [5].

References

[1] C. Esmersoy. Inversion by reverse-time extrapolation and a new imaging principle. In *Soc. Expl. Geophys., Expanded Abstracts*, pages 608–611s, 1986.

[2] S. Geoltrain and J. Brac. Can we image complex structures with first-arrival traveltime? *Geophysics*, 58:564–575, 1993.

[3] O. Holberg. Towards optimum one-way wave propagation. *Geophys. Prosp.*, 36:99–114, 1988.

[4] G. A. McMechan. Migration by extrapolation of time-dependent boundary values. *Geoph. Prosp.*, 31:413–420, 1983.

[5] A. P. E. Ten Kroode, D. J. Smit, A. R. Verdel. A microlocal analysis of migration. *Wave Motion*, 28:149–172, 1998.

[6] J. W. Thorbecke and W. E. A. Rietveld. Optimum extrapolation operators – a comparison. In *Expanded Abstracts*. Eur. Ass. of Expl. Geoph., 1994.

[7] C. P. A. Wapenaar and F. J. Herrmann. True amplitude migration taking fine-layering into account. In *Soc. Expl. Geophys., Expanded Abstracts*, pages 653–656, 1993.

[8] C. P. A. Wapenaar, G. L. Peels, V. Budejicky, and A. J. Berkhout. Inverse extrapolation of primary seismic waves. *Geophysics*, 54(7):853–863, 1989.